Gas Processing Journal

Vol. 3, No.2 , 2015
http://uijs.ui.ac.ir/gpj

Improvement of Overall Efficiency in the Gas Transmission Networks: Employing Energy Recovery Systems

Sahar Safarian*[1], Maryam Mousavi[2]

[1,2] Department of Energy Engineering, Sharif University of Technology, Tehran, Iran

Abstract: This study mainly focuses on enhancing the overall efficiency of gas transmission networks. The authors developed a model with detailed characteristics of compressor and pressure reduction stations. Following this, they suggested three different systems with gas turbine including: organic rankine cycle (ORC), air bottoming cycle (ABC), and ABC along with steam injection (SI-ABC). In addition, use of turbo-expander as a good alternative to the expansion valves was also studied. Performance of proposed cycles was investigated on a real case study for natural gas transmission network. Results showed that the highest efficiency would be obtained with ORC system where n-pentane was used as the working fluid and turbo-expander was considered in pressure reduction stations Moreover, the efficiency improvement was estimated to be 22% averagely in comparison with the existing network where the flow was in the span of 50 up to 90 MMSCMD.

Keywords: Natural Gas Transmission Network, Organic Rankine Cycle, Air Bottoming Cycle, Steam Injection Air Bottoming Cycle, Turbo-Expander, Overall Efficiency.

1. Introduction

Natural gas is one of the most widely used sources of energy in the world due to its environmental issues and global warming concerns. As such, the demand for natural gas, as a primary energy, are increasing more and more. It is predicted that the natural gas demands increase at an average rate of 2.4 percent annually until 2030 in the world (Najibi & Taghavi, 2011). Normally, the locations of natural gas resources and end points for various applications are far apart. As a result, it must be transformed from the deposit and production sites to the consumers through the pipeline networks. Increasing the natural gas demands and pipeline networks requires focus on the overall efficiency of transmission. Currently, it is low because much of energy is wasted in the transmission network; these energies are recoverable. Consequently, the development of high efficiency gas transmission network is a key issue in order to satisfy the growing demand from the various customers (Guo & Ghalambor, 2014).

In the transmission network, gas flows through pipes and various devices such as regulators, valves, and compressors. The gas pressure is reduced mainly due to wall friction and also heat transfer between the gas and the surroundings. Hence, compressor stations should be installed to boost the gas pressure and keep it moving to the desired destinations. Gas compression is usually performed using the centrifugal or reciprocating compressors driven by the gas turbines or the electrical motors. Gas turbines are more common because of several reasons. First of all, their operating cost is lower than the electrical motors. Secondly, installation cost of a new interconnecting electric power transmission line may be high. Finally, it may be difficult to obtain the necessary regulatory approvals for the electrical motors. However, it is estimated

* Corresponding Author.
Authors' Email Address:
[1] Sahar Safarian (safarian@energy.sharif.edu),[2] Maryam Mousavi (maryam_mousavi88@yahoo.com)

ISSN (On line): 2345-4172, ISSN (Print): 2322-3251

that 3-5% of the transported gases are consumed by the gas turbines as fuel (Borraz-Sánchez & Ríos-Mercado, 2005; Wu, Rios-Mercado, Boyd, & Scott, 2000) and the exhaust gases from turbines with high temperature are released into the environment which leads to the serious environmental pollution(Dai, Wang, & Gao, 2009).

After passing all compression stations, the gas pressure must be reduced at distribution points. Currently, most pressure reduction stations use expansion valves, which may waste lots of energy associated with high pressure gas. Hence, energy recovery from pressure compression and reduction stations can be regarded as one of the focal points to improve the overall efficiency of gas transmission network.

Edgar et al. (Edgar, Himmelblau, & Bickel, 1978), Cobos-Zaleta et al. (Zaleta & Ríos-Mercado, 2002), Ríos-Mercado et al. (Ríos-Mercado, Kim, & Boyd, 2006), Kabirian et al. (Kabirian & Hemmati, 2007) and Safarian et al. (Safarian, Saboohi, & Kateb, 2013) presented different models or various procedures to optimize the gas transmission network. The objective of their models was to minimize the cost or energy consumption of transmission system. The effect of pressure reduction station and the function of energy recovery from current gas transmission network were not considered in their work.

In the current study, minimizing the energy consumption and maximizing the flow rate through the pipes were the basic issues of this study and the main objective of this research was to maximize energy recovery and excess power by utilizing different technologies on the compression and reduction stations. Evaluation of various technologies such as turbo-expander, organic rankine cycle, air bottoming cycle, and steam air bottoming were conducted in the literature (Cho, Cho, & Kim, 2008; Maddaloni & Rowe, 2007); It is worth mention that, this research study, investigating all these systems together, presents a comprehensive model to compare them. Following the most efficient system can be identified.

In 2007, Maddaloni and Rowe investigated the application of turbo expander in the gas pressure reduction station to produce electricity. The electricity could either be routed back into the electric distribution grid or used to produce small amounts of hydrogen. They found that at their assumed peak efficiencies, electricity could be extracted from the pressure reduction system with 75% exegetic efficiency, and hydrogen could be produced with 45% energetic efficiency.

In the compression stations, one common solution for increasing the performance of a gas turbine is to combine it with a steam cycle or with an organic rankine cycle. This can be used either to generate electricity alone, or to co-generate both electric power and heat for industrial and home purposes (Safarian & Bararzadeh, 2012).

Due to lower vaporization heat, organic fluids are preferred to water; this is critical especially when the available power and the heat source temperature are low. In this situation, these fluids can better follow the heat source to be cooled; this reduces the temperature differences and therefore, irreversibilities at the evaporator. Furthermore, the turbines for organic cycles could provide higher efficiencies at partial loads. In addition their complexity is usually less due to the lower enthalpy drop of the fluid(Drescher & Brüggemann, 2007; Larjola, 1995).

In 2009, Desai et al. (Desai & Bandyopadhyay, 2009) proposed a methodology for accurate optimization of an ORC as a co-generation process to generate shaft-work, with16 different organic fluids. In addition, they investigated the benefits of integrating ORC with the background process and reported on the applicability of proposed methodology with illustrative examples.

In 2010, Roy et al. (Roy, Mishra, & Misra, 2010) performed parametric optimization and performance analysis of a waste heat recovery system along with Organic Rankine Cycle to generate the power. This analysis was performed for R-12, R-123, and R-134a as working fluids. They also found that R-123 had the maximum work output and efficiency among all the selected fluids.

Combining the gas turbine cycle with an air bottoming cycle (ABC) is another method that has been found to increase the performance of a gas turbine (Korobitsyn, 1998). In1995, Kambanis (Kambanis, 1995) and in 1996, Bolland (Bolland, Forde, & Hande, 1996), reported that by using the exhaust gas of a simple gas turbine in the air bottoming cycle the efficiency of the combined cycle improved about 47% and 46.6% respectively.

In the recent study, Ghazikhani et al. (Ghazikhani, Passandideh-Fard, & Mousavi, 2011) developed a model for the steam injection in the gas turbine with air bottoming cycle. They also found two new cycles with ABC. These cycles were: the Evaporating Gas turbine with Air Bottoming Cycle (EGT-ABC), and Steam Injection Gas turbine with Air Bottoming Cycle (STIG-ABC). Their findings indicated that EGT-ABC had a lower irreversibility and higher output compared to the STIG-ABC.

In this article, the authors developed a model for the technical analysis of transmission network considering characteristics for pressure compression and reduction stations and the energy recovery technologies. The developed model estimated net possible output power, overall efficiency and system energy loss to evaluate the performance of the gas transport networks. It is should be noted that, the model utilized equations of real gases for estimation of enthalpy which produced accurate results no longer needing Moulier graphs.

2. Methodology

2.1. Definition of Transportation Efficiency

Transportation efficiency can be regarded as a function of the overall system design, the efficiency of individual components, and the way that the system is operated. Transportation efficiency is defined as the amount of fuel burned or electric power used per unit of the throughput (i.e., British thermal unit (Btu) or kW/Mcf). In addition to this general definition, there are three other related measures.

1. Hydraulic efficiency is a measure of the loss of energy (pressure drop) caused by the friction of the flowing gas in the pipeline facilities.
2. Thermal efficiency applied to a prime mover (engine, turbine or motor), t measures as fraction of the potential energy of an input fuel or electric power which is converted into useful energy; this energy can be used to drive a compressor. The amount of energy that is not converted into useful energy is considered as “waste heat” in the exhaust.
3. Compressor efficiency measures how much energy is expended in compressing the gas compared in comparison with overall energy used by the compressor. Inefficient compressors heat the gas instead of raising its pressure and thus have lower efficiency values.

2.2. Proposed Model

The model was developed for the existing gas pipelines networks from supply to demand nodes. The demand nodes were major locations of natural gas consuming in the study area. The demand nodes were either consumption regions in the study area or export terminals of natural gas from the study area to the outside. In contrast, supply nodes were resources locations for natural gas processing in the study area. These nodes included either refineries, natural gas producing plants, or the import terminals of natural gas from the outside of the study area (Safarian et al., 2013). In addition the model considered all network units i.e. gas compressor, air compressor, gas turbine, combustion chamber, expansion valves and heater in the compressor stations, and pressure reduction stations.

The model consisted of four sub-models that are defined below:

1. Base scenario,
2. Reduction stations along with turbo-expander,
3. Compression stations affixed to ORC,
4. Compression stations affixed to ABC and SI-ABC

The main thermodynamic assumptions that were used in the present analysis are reported in Table 1.Second Iran gas transmission network was chosen as the case study in this work. This network with 7 major compression stations was one of the most important network systems in Iran.

Table 1. Conditions and Assumption Used in the Calculation

Thermodynamic Assumptions	
Isentropic compressor efficiency	88%
Combustion chamber pressure drop	3%
Isentropic turbine efficiency	90%
Turbine mechanical efficiency	99%
Compressor mechanical efficiency	99%
Regenerator effectiveness	85%
Regenerator pressure drop (hot fluid)	2%
Regenerator pressure drop (cold fluid)	2%
HRSG efficiency	75%
HRSG pressure drop (water and steam)	6%
HRSG pressure drop (flue-gas)	2%
Pump efficiency Hydraulic	80%
Expander efficiency	75%
Gearbox efficiency	92%
Generator efficiency	95%

2.3. Base Scenario

In this scenario, gas transmission network is considered without energy recovery and it includes simple pressure compression and reduction stations. In this sub-model, the aim is to minimize the energy used in the gas compressors. This can be written as following (O'Neill, Williard, Wilkins, & Pike, 1979):

$$\min z = \alpha \sum_j \frac{1}{0.9\eta_{therm}} W_j \tag{1}$$

Where α is the unitary energy price ($/kW), η_{therm} is the compressor thermic efficiency and W_j is compressor required power that is calculated by (Menon, 2005):

$$W_j = 4.0639 T_1 Q \left[\frac{\gamma}{\gamma-1}\right] \left[\frac{Z_1+Z_2}{2}\right] \left[\frac{1}{\eta_a}\right] \left[\left(\frac{P_2}{P_1}\right)^{\frac{\gamma}{\gamma-1}} - 1\right] \tag{2}$$

Where T_1, P_1 and Z_1 are input temperature, pressure and compressibility factor and T_2, P_2 and Z_2 are output ones, respectively. η_a stands for the compressor adiabatic efficiency, Q is gas flow rate through the pipeline (MMSCMD) and γ is the ratio of specific heats which assumed to be constant.

According to Weymouth equation (equation 3), based on the input conditions, designed maximum and minimum pressure and type of pipe material, the maximum flow rate through the pipeline must be calculated. Considering this, the demand should always be lower than maximum flow rate to satisfy the restrictions for flow capacity.

$$Q = 3.7435\times10^{-3} E \left[\frac{T_b}{P_b}\right] \left[\frac{P_1^2 - e^s P_2^2}{G L_e Z T_{ave}}\right]^{0.5} D^{2.667} \tag{3}$$

$$L_e = L\frac{(e^s-1)}{s} \tag{4}$$

$$s = 0.0684G\left[\frac{H_2-H_1}{ZT_f}\right] \tag{5}$$

Also, at each end point, the demand must be guaranteed at a minimal pressure. On the other hand, the gas transmission company cannot take gas at a pressure higher than predefined value. Mathematically (O'Neill et al., 1979):

$$P_{i,min} \leq P_i \leq P_{i,max} \tag{6}$$

Fig. 1 shows a schematic of gas compression station. The inlet air enters the compressor at state1. Considering an isentropic efficiency of η_{comp} for the compressor and a constant pressure ratio of r_c that can be calculated as:

$$r_c = \frac{P_2}{P_1} \tag{7}$$

Because of high pressure of the inlet natural gas, the reduction valve must be used. At the next step, compressed air combusts with medium pressure fuel. Consequently, exhaust gases exit from combustion chamber and enters the turbine. At final state, turbine output work is obtained which depends on exhaust temperature (TIT) and mass flow. Turbine output power could be estimated from equation 2 but, the outcome of this equation was not accurate. To have accurate value of outcome, equation of states for real gases was used in our model as follows (Abbott, Smith, & Van Ness, 2001)

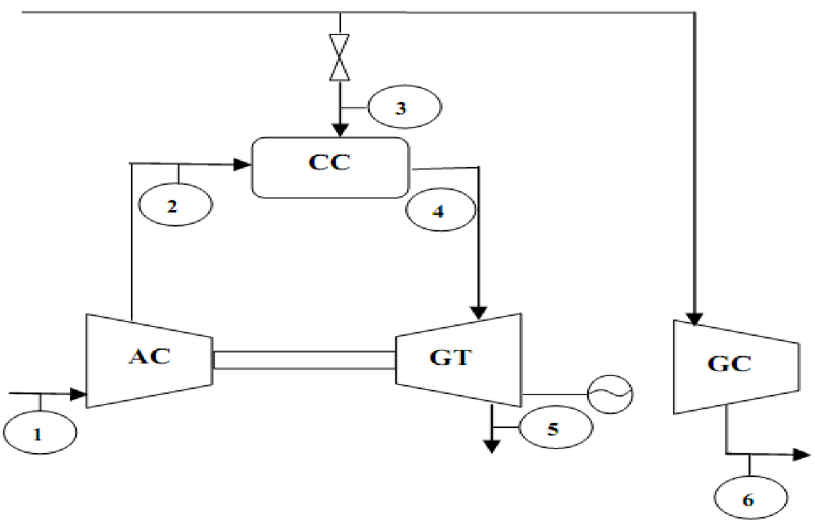

Figure 1. Schematic Diagram of Gas Compression Station

$$\dot{W}_{gas\ comp} = \dot{m}_{NG}(h_7 - h_6) \quad (8)$$

Which:

$$H = H_0^{ig} + \int_{T_0}^{T} Cp^{ig} dT + H^R \quad (9)$$

Every component has unique value of H_0^{ig}; for example this is -74920 (kJ/kgmol) for methane. Second part of equation 9, can be simplified to:

$$\int_{T_0}^{T} Cp^{ig} dT = (Cp^{ig})_H \times (T - T_0) \quad (10)$$

$$(Cp^{ig})_H = R(A + \frac{B}{2} T_0 \left(\frac{T}{T_0} + 1\right) + \left(\left(\frac{T}{T_0}\right)^2 + \frac{T}{T_0} + 1\right) \times \frac{C}{3} T_0^2 + \frac{D}{T_0} T) \quad (11)$$

Table 2, shows all constants for calculation of methane specific heat. Last part of equation 9, is called residual enthalpy which appears when natural gas is assumed to be real not ideal, and also gas pressure is more than atmospheric.

Table 2. Methane Constants

constants	value
A	1.702
B	9.081e-3
C	-2.164e-6
D	0
T_C (K)	190.6
P_C (Kpa)	4599000

$$\frac{H^R}{RT} = Z - 1 + \left(\frac{dLna(T_r)}{dLnT_r} - 1\right) qI \quad (12)$$

$$q = \frac{a(T)}{bRT} \quad (13)$$

$$I = \frac{\beta(T,P)}{Z + \varepsilon\beta} \quad (14)$$

$$a(T) = c\,(1 + (0.37464 + 1.54226\,w - 0.26992\,w^2)\ (1 - \sqrt{T_r}))^2 \quad (15)$$

Where Z, T_r and w are gas compressibility factor, reduced temperature and acentric factor, respectively.

In the same way, the power for other units in compression station is shown below:

$$\dot{W}_{air\ comp} = \dot{m}_{air}(h_2 - h_1) \quad (16)$$

$$\dot{W}_{gas\ turb} = \dot{m}_{flugas}(h_4 - h_5) \quad (17)$$

$$\dot{W}_{net} = \dot{W}_{gas\ turb} - \dot{W}_{gas\ comp} - \dot{W}_{air\ comp} \quad (18)$$

The other parameter which is different in real and ideal gasses is entropy. Regarding this, entropy for real gas can be written as:

$$S = S_0^{ig} + \int_{T_0}^{T} Cp^{ig} \frac{dT}{T} + S^R - RLn\frac{P}{P_0} \quad (19)$$

S_0^{ig} is the standard entropy of ideal gas that is constant for each component and it is 183.48 (kJ/kgmol.K).for methane.

$$\frac{S^R}{R} = Ln(Z - \beta) + \frac{dLna(T_r)}{dLnT_r} \times q \times I \quad (20)$$

Passing all compression stations, near demand nodes, the gas enters to gas pressure reduction stations. The process that currently performs in reduction stations is shown in Fig. 2. At the first stage gas enters to the heater to make up reducing temperature during expansion process and then it passes under the constant enthalpy process in Joule-Thomson valves.
The model estimates dissipation rate of pressure energy in the expansion valves, required amount of heat and total loss of energy in the reduction stations. The result of this part provides us a general overview about the amount of energy which is being wasted in gas pressure reduction stations. This can be written:

$$Energy\ Loss = T_0 Q(C_P \left(Ln\frac{T_3}{T_2}\right) - (R(Ln\frac{P_3}{P_2}))) \quad (21)$$

$$Required\ Heat = \dot{m}_{NG}(h_2 - h_1) \quad (22)$$

2.4. Affix of turbo-expander to reduction stations

In this part, the authors considered using turbo-expander instead of J-T valves. For this purpose, they develop model to calculate output power and required heat of turbo-expander system. Fig. 3 shows a simple schematic of an improved station.

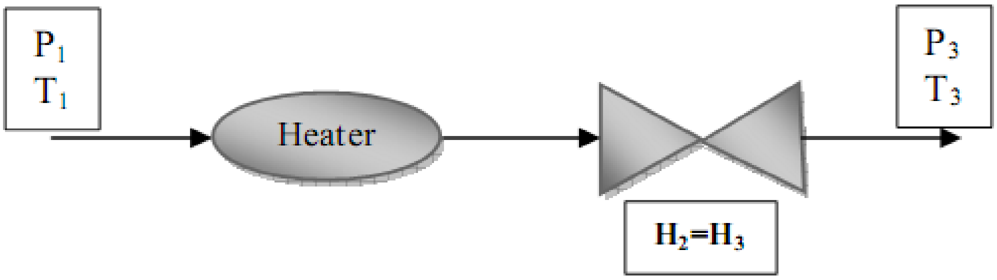

Figure 2. The Schematic of the Conventional Reduction Station

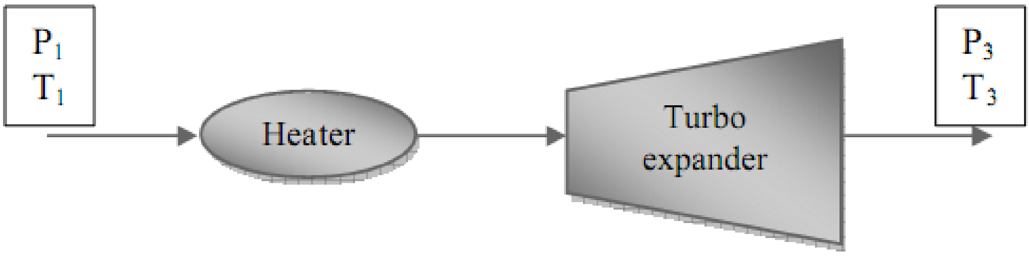

Figure 3. The Schematic of the Improved Reduction Station

Equations 9-15, 19 and 20 are the base equations in this part. Inlet conditions of heat exchanger and outlet conditions from turbo expander are key inputs. Considering an isentropic efficiency of η_{exp} for the expander and pressure drop of 1.46(%) during heater.
The most important operational challenge in the turbo-expander is hydrate formation due to the slight amount of water in the gas. Two factors which are intensified hydrate formation are the low temperature and high pressure. So a proper temperature for outlet heat exchanger should be found out considering this phenomenon. At the first step, the expander is considered as isentropic process and then using trial and error for T_2 and equation of expander efficiency, the model estimates the correct answer for T_2.

$$\eta_{exp} = \frac{H_2 - H_3}{H_2 - H_{3s}} \tag{23}$$

The output power and required heat can be obtained as follows: Having considered the heat exchanger pressure drop, turbo-expander efficiency, fuel mass flow rate and generator and gearbox efficiency, we can have:

$$\dot{W}_{exp} = \dot{m}_{NG}(h_2 - h_3).\eta_{GB}.\eta_{Gen} \tag{24}$$

$$\dot{Q}_{Hex} = \dot{m}_{NG}(h_2 - h_1) \tag{25}$$

The thermodynamic properties of natural gas are used in the model and the procedure of model solution is given in flow chart1 in the Appendix.

2.4.1. Validation

To validate the first sub-model, the results of the model were compared to those of the experiments performed by Pozivil (Poživil, 2004) (Fig 4) and also to the simulation results (Fig 5 and 6). For the output power and heat duty against temperature inlet expander and inlet flow of natural gas, a good agreement was observed. The discrepancy between the two results is less than 6%.

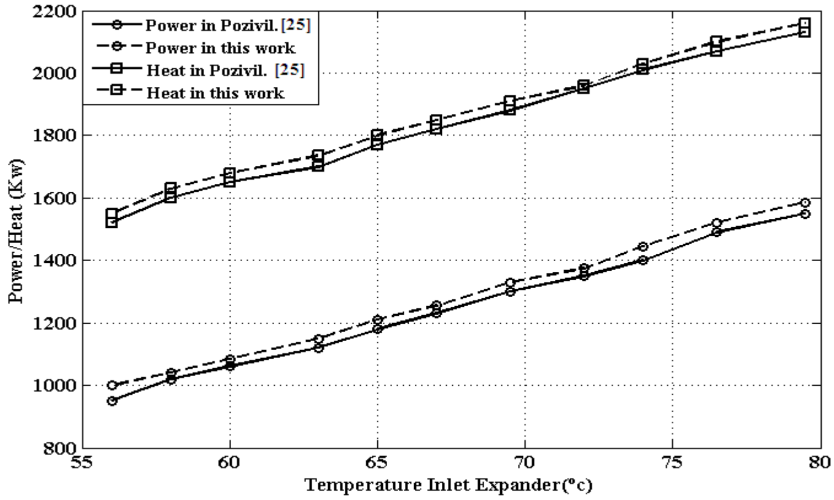

Figure 4. Comparison of Model Results with those of Pozivil. [22] for the Turbo-Expander

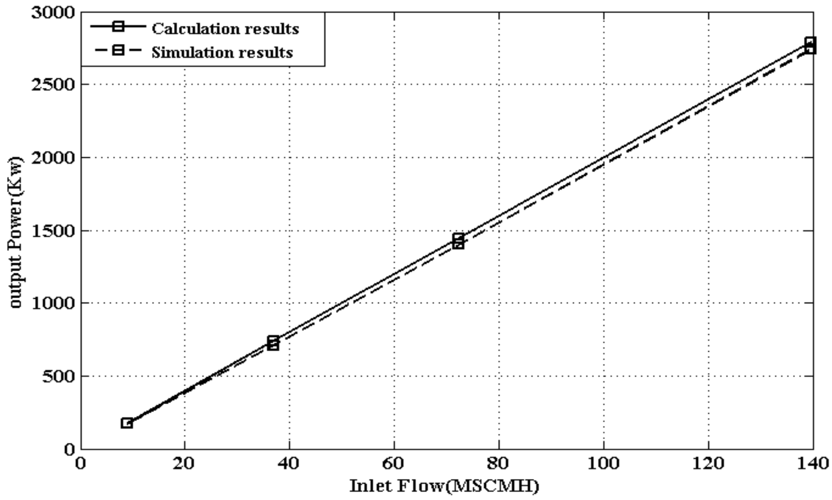

Figure 5. Comparison of the Results of Eexpander Power with the Simulation Results (P_1=4466 Kpa, p_3=1825 Kpa, T_1=30 $^{\circ}C$ and T_3=18 $^{\circ}C$)

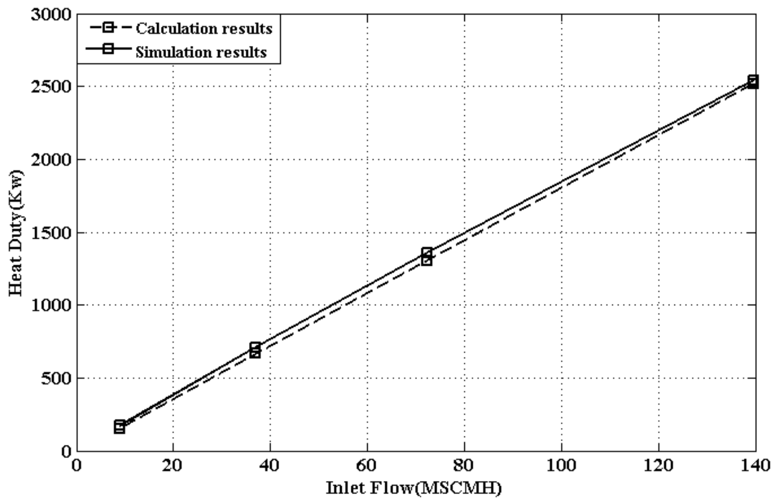

Figure 6. Comparison of the Results of Heat Duty with the Simulation Results (P_1=4466 Kpa, p_3=1825 Kpa, T_1=30 $^{\circ}C$ and T_3=18 $^{\circ}C$)

2.4.2. Sensitivity Analysis

A sensitivity analysis was conducted in order to better understand the effect of key-parameters of process performance. In this analysis, the effect of an additional percentage of parameters P_1, T_1 and flow rate on the output power and heat duty were investigated using the model. The expander outlet pressure and temperature were 1825 kpa and 18°C, respectively.

Fig. 7 and 8 show the details of the sensitivity analysis. Two figures are plotted for the capacities of 37, 139.73 and 371 MSCMH.

As seen in Fig. 7, although output power and required heat had a direct relationship with inlet pressure and flow when inlet pressure was close to outlet pressure, the expansion system efficiency will be greater due to the low difference between two graphs.

$$\eta_{\text{turbo - ex sys}} = \frac{\text{output power}}{\text{required heat}} \tag{26}$$

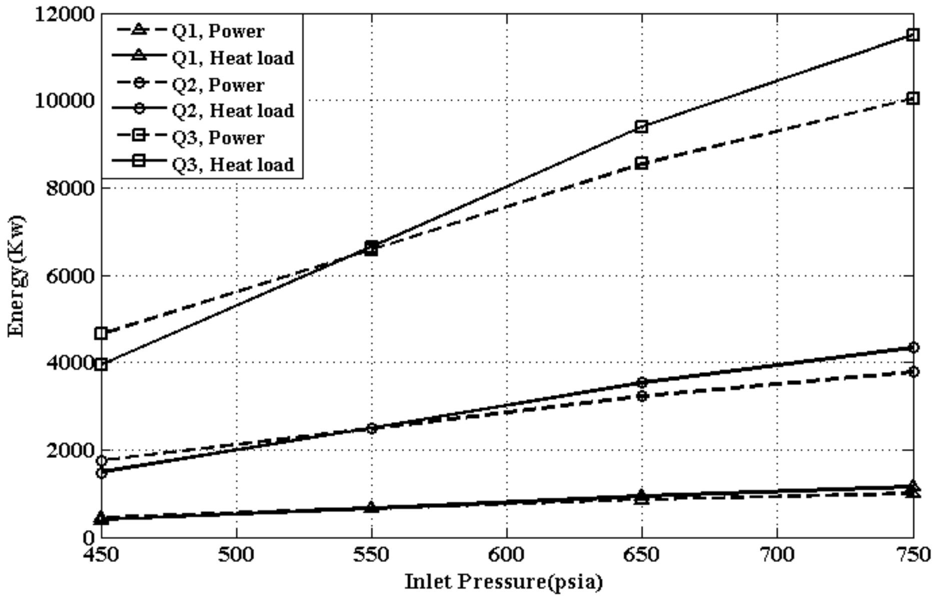

Figure 7. The Effect of Inlet Pressure on Energy for Different Capacities (Q_1=37, Q_2=139.73, Q_3=371 MSCMH, T_1=30 $^{\circ}C$, P_3=1825 Kpa, T_3=18 $^{\circ}C$)

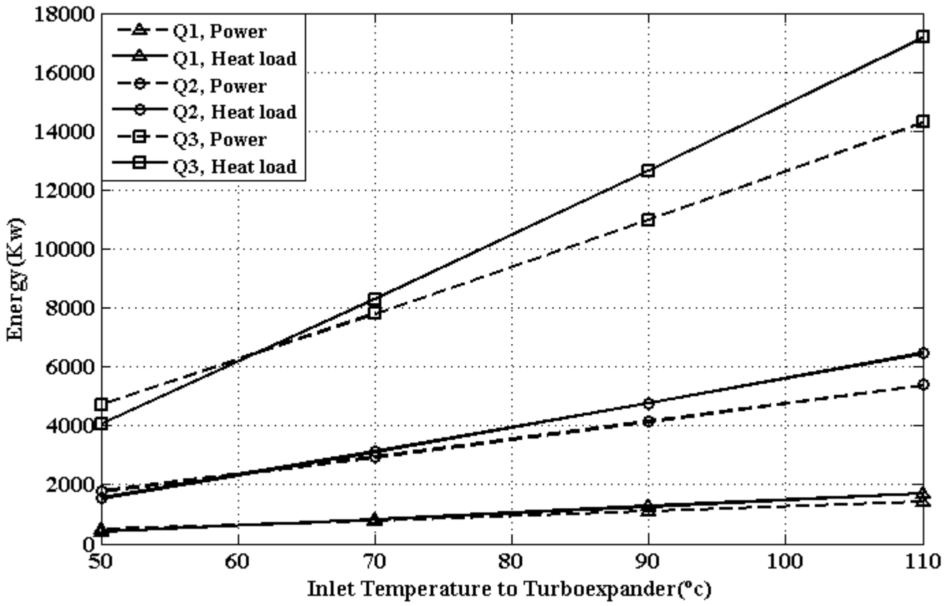

Figure 8. The Effect of Inlet Temperature on Energy for Different Capacities (Q_1=37, Q_2=139.73, Q_3=371 MSCMH, P_1=4466 Kpa, T_1=30 $^{\circ}C$, P_3=1825 Kpa, T_3=18 $^{\circ}C$)

It is evident in Fig. 8 that expander power and heat duty were more sensitive to inlet temperature. Following this, with using boiler in maximum load, more power would be obtained without the extra cost. In addition, there was a specific temperature for each inlet pressure where output power and required heat were equal; on the other hand expansion system efficiency is 100%.

2.5. Affix of ORC to Compression Stations

2.5.1. Thermodynamic Analysis of ORC

The ORC system consisted of an evaporator, turbine, condenser and pump. It could be classified into two groups according to the level of turbine inlet pressure, including supercritical ORCs and sub-critical ORCs (Safarian & Aramoun, 2015). In the present study, the sub-critical ORCs were investigated.

As is shown in Fig. 9, the working fluid left the condenser as saturated liquid (point1). Then, it was compressed by the liquid pump to the sub-critical pressure (point2). The working fluid was heated in the evaporator until it became superheated vapor (point3). In this research, heating process to working fluid was considered to be indirect. In other words, an inductor fluid such as oil over took heat transfer to working fluid. The reason of this was to increase the security and management level of process. The superheated vapor flowed into the turbine and expanded to the condensing pressure (point4), and then, the low pressure vapor led to the condenser and condensed by air. The condensed working fluid flew in to the receiver and was pumped back to the evaporator, and a new cycle began.

In the mentioned cycle, if the temperature T_4 was considerably higher than the temperature T_1, it might be useful to implement an internal heat exchanger (IHE) into the cycle as shown in Fig.10.This heat exchanger is also depicted in Figs.9 by the additional state points 4a and 2a. The turbine exhausts flowed in to the internal heat exchanger and cool in the heat exchanger in the process (4–4a) by transferring heat to the compressed liquid that was heated in the process (2–2a)(Vaja & Gambarotta, 2010).

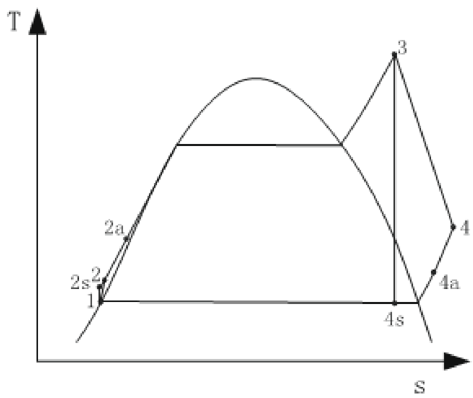

Figure 9. T-S Diagram of ORCs

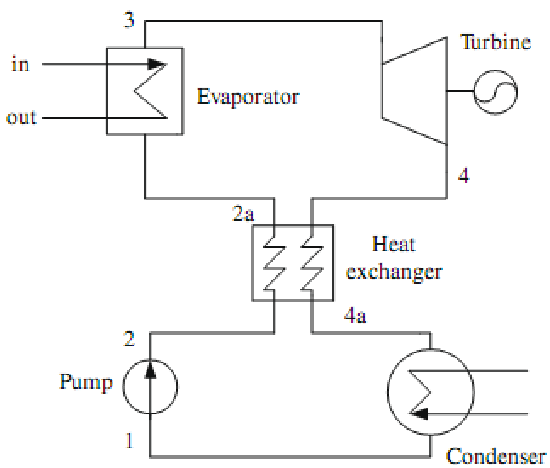

Figure 10. The ORC System with Internal Heat Exchanger

Each process in the ORC can be described as follows:
Process 2 to 3: This was the heat absorption process in the evaporator. The pressure drop due to evaporation was considered. The amount of heat transferred from the waste heat to the working fluid is (Wei, Lu, Lu, & Gu, 2007):

$$\dot{Q} = \dot{m}_{flugas}(C_{Pin}T_{in} - C_{Pout}T_{out}) \quad (27)$$

or

$$\dot{Q} = \dot{m}_{wf}(h_3 - h_2) \quad (28)$$

If the internal heat exchanger is added, the amount of heat transfer can be calculated by:

$$\dot{Q} = \dot{m}_{wf}(h_3 - h_{2a}) \quad (29)$$

Process 3 to 4: This was a non-isentropic expansion process in the turbine. Ideally, this was an isentropic process 3–4s. However, the efficiency of the energy transformation in the turbine never reached 100%, and the state of the working fluid at the turbine outlet is indicated by state point 4. The isentropic efficiency of the turbine can be expressed as:

$$\eta_{turb} = \frac{h_3 - h_4}{h_3 - h_{4s}} \quad (30)$$

The power generated by the turbine can be given as:

$$\dot{W}_{wf\,turb} = \dot{m}_{wf}(h_3 - h_4) \quad (31)$$

Process 4 to 1: This was a constant pressure exothermic process in the condenser.
Process 1 to 2: This was a non-isentropic compression process in the liquid pump. The isentropic efficiency of the pump can be expressed as:

$$\eta_{pump} = \frac{h_{2s} - h_1}{h_2 - h_1} \quad (32)$$

The input work by the pump is:

$$\dot{W}_{wf\,pump} = \dot{m}_{wf}(h_2 - h_1) \quad (33)$$

The thermal efficiency of the ORC is defined on the basis of the first law of thermodynamics as the ratio of the net power output to the added heat.

$$\eta_{thm} = \frac{\dot{W}_{wf\,turb} - \dot{W}_{wf\,pump}}{\dot{Q}} \quad (34)$$

The procedure of model solution is given in Flow chart 2 in the Appendix.

2.5.2. Validation

To validate the model, the results of the model were compared to those of the experiments performed by Dai et al. (Dai et al., 2009). Fig. 11 shows a comparison of model results with these experiments for 3 different working fluids. Fig. 11 shows net power output against turbine inlet temperature where a good agreement is observed. The discrepancy between the two results was less than 5%. Although as the turbine inlet temperature increased, the net output power for ammonia and water increased correspondingly, for the butane, an increase in turbine inlet temperature led to a reduction in net output power. For instance when TIT varied from 90 to 135 (°C) the efficiency of ORC-butane decreased by 7.9 % averagely, although it was increased by 7.2 % and 2.1 % for ammonia and water, respectively. Consequently, for high TIT ammonia was better choice among these three working fluids.

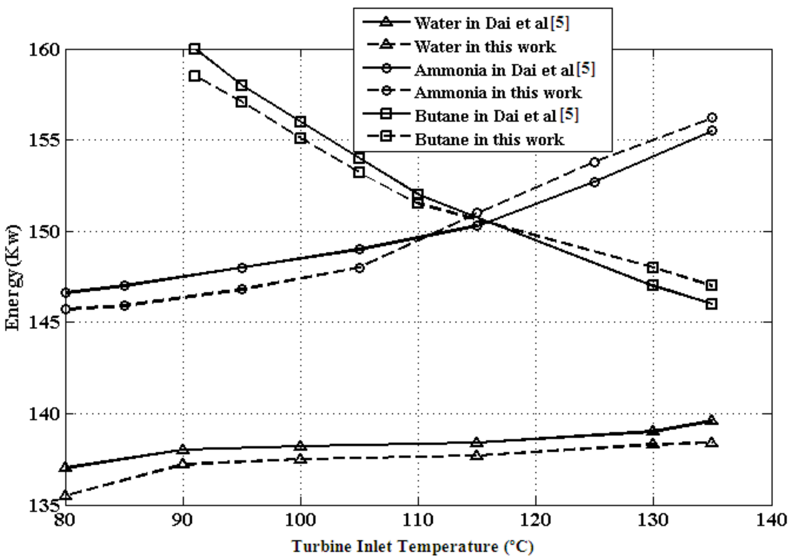

Figure 11. Comparison of Model Results with those of Dai et al. [24] for the ORCs

2.5.3. Sensitivity Analysis

A sensitivity analysis was conducted for n-pentane as working fluid to better understand the effect of parameters on the process performance. Fig.12 shows the effect of gas turbine outlet temperature on output power of n-pentane turbine and ORCs efficiency. The output work was increased by increasing flu gas temperature, because more amount of n-pentane could be evaporated by this way. But the ORCs efficiency was decreased due to the increase in Q in equation 34.

As seen in Fig.13 the obtainable work was grown by increment of flu gas rate, because of increase in heat absorption process in the evaporator. The net output power was enhanced too. In addition, Fig.13 shows a changeless trend for ORCs efficiency because the ratio of increase of net output power and required heat were kept constant.

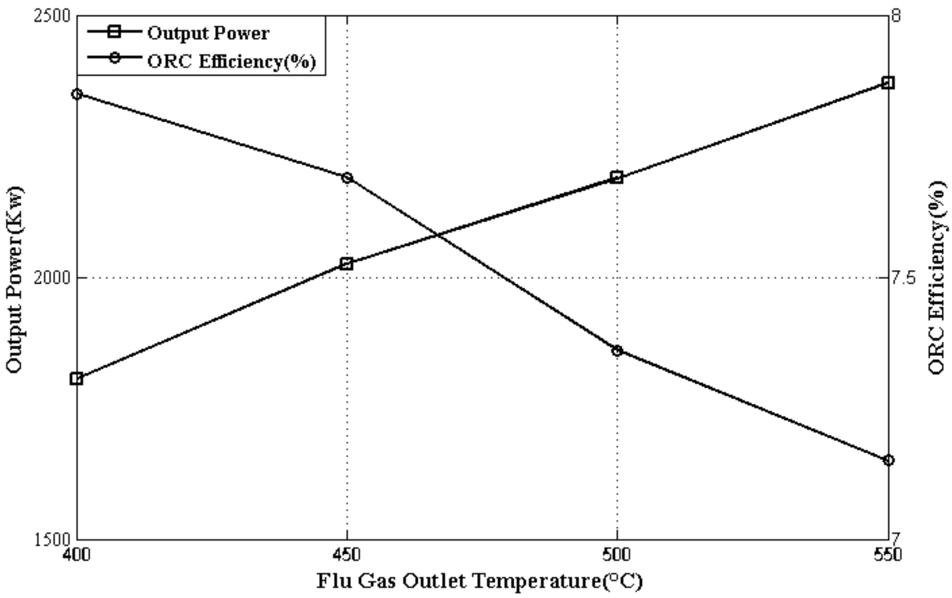

Figure 12. The Overall Efficiency and Output Power Variation against Flu Gas Outlet Temperature

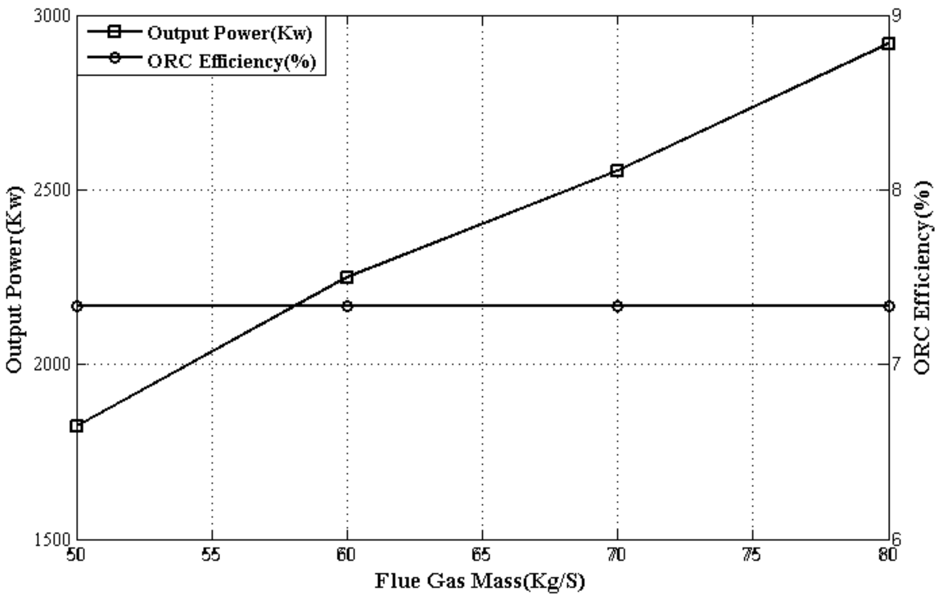

Figure 13. The Overall Efficiency and Output Power Variation against Flu Gas Mass

The effect of n-pentane turbine inlet pressure on net output power and ORCs efficiency at constant inlet temperature (490°C) is displayed in Fig.14. The net output power and ORCs efficiency were augmented by increasing of inlet pressure.

2.6. Affix of ABC and SI - ABC to Compression Stations

An Air Bottoming Cycle system consists of an air compressor, regenerator and turbine. Fig.15 shows such a combined cycle in which the exhaust of an existing, topping gas turbine was sent to a gas-air heat exchanger which heated the air in the secondary gas turbine cycle.

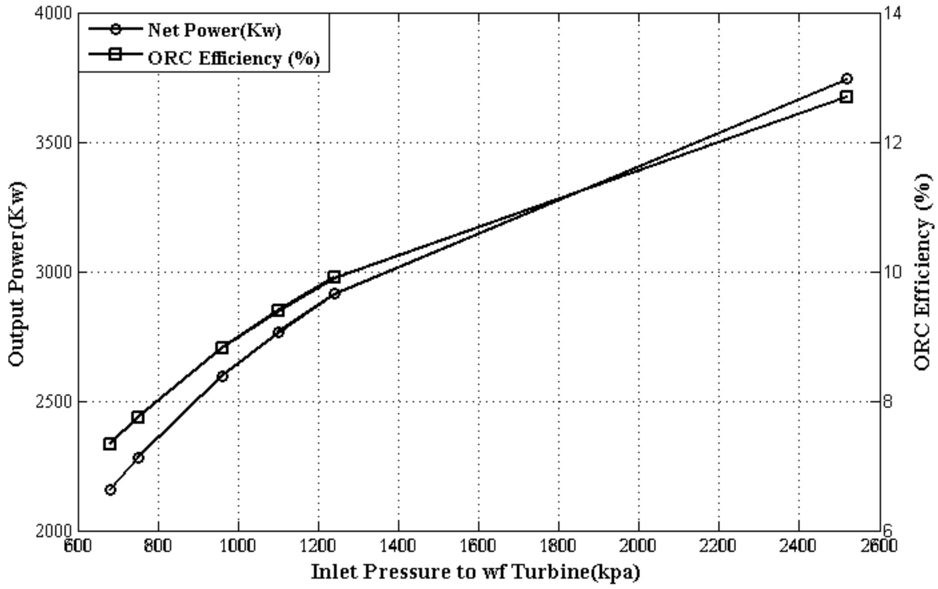

Figure 14. The Overall Efficiency and Output Power Variation against Turbine Inlet Pressure

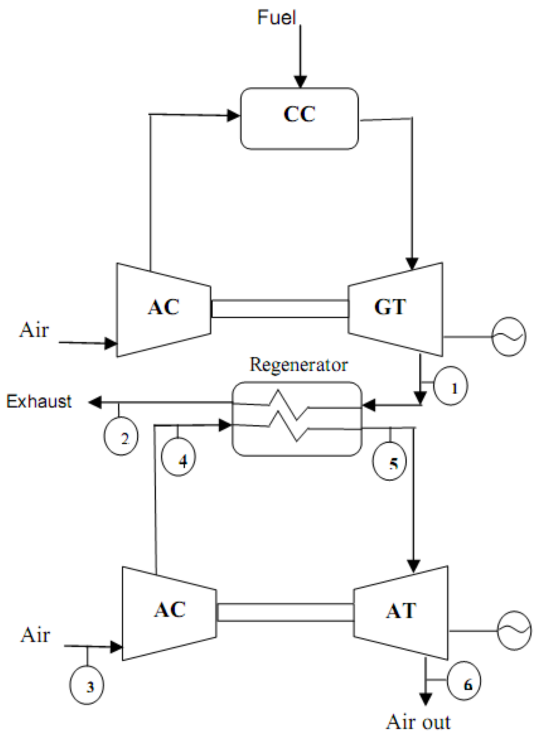

Figure 15. Gas Turbine with Air Bottoming Cycle.

ABC was proposed in the late 1980s as an alternative for the conventional steam bottoming cycle. Nowadays, this cycle was considered as a compact and simple bottoming cycle in the various applications: as an upgrading option for simple-cycle gas turbines in the offshore industry, a hot-air co-generation plant, and a heat recovery installation at high-temperature furnaces.

Fig.16 also shows Steam Injection Gas Turbine with Air Bottoming Cycle (SI-ABC). The topping exhaust gases had high temperature after passing through the regenerator. Thermal energy of these gases could be used for evaporating of water. The steam was then mixed with ABC compressor discharged air in a mixer (Ghazikhani et al., 2011). The evaporating process was performed in the HRSG. The temperature of the exhaust gas was decreased in about 120 °C by generating steam. The amount of the injected steam per unit fuel flow is 5-6 (kg/kg-fuel) (Nishada, Takagi, & Kinoshita, 2005)

The model developed in this study included the calculation of three cycles: simple gas turbine, ABC, and SI-ABC. Each process in the ABC can be described as follows:

Process 1 to 2: This was the heat absorption process in the regenerator. The pressure drop due to regenerator was considered. Enthalpy of flu gas was calculated by equations 9-15. Equation 35 is utilized for estimation of air outlet temperature from regenerator.

$$\varepsilon_{reg} = \frac{C_1(T_1 - T_2)}{C_{min}(T_1 - T_4)} \tag{35}$$

Process 3 to 4: The inlet air entered the compressor at state 3. The compressor inlet power was calculated as:

$$\dot{W}_{air\,comp} = \dot{m}_{air}(h_4 - h_3) \tag{36}$$

Air outlet temperature from regenerator was the function of outlet enthalpy which can be estimated by energy balance equation around regenerator.

$$\dot{m}_{flugas}(h_1 - h_2) = \dot{m}_{air}(h_5 - h_4) \tag{37}$$

Process 5 to 6: This was a non-isentropic expansion process in the turbine. The isentropic efficiency of the turbine can be expressed as:

$$\eta_{turb} = \frac{h_5 - h_6}{h_5 - h_{6s}} \tag{38}$$

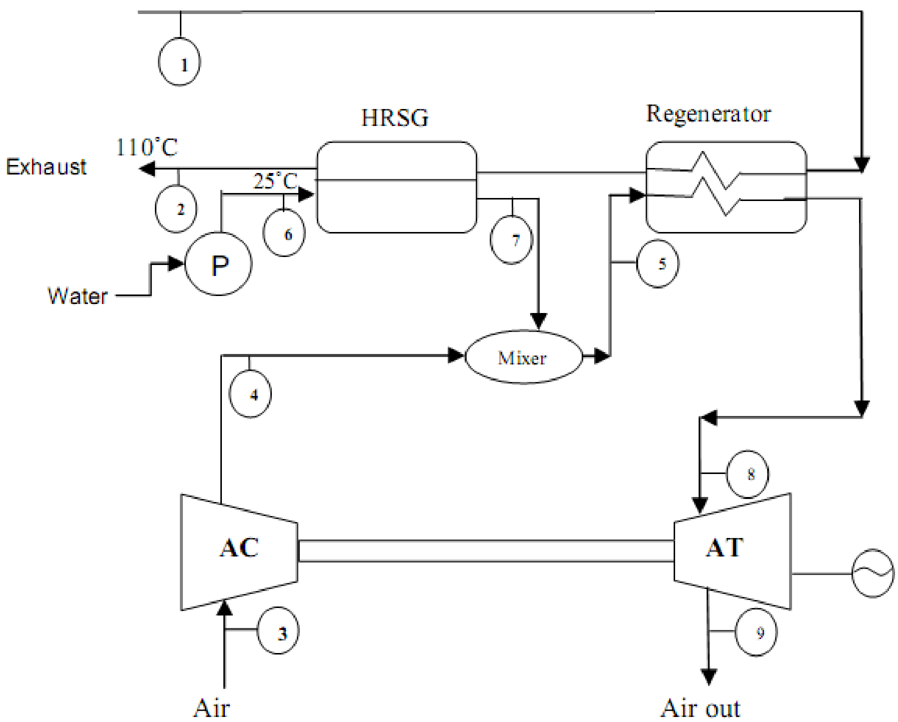

Figure 16. Steam Injection with Air Bottoming Cycle

The power generated by the turbine can be given by:

$$\dot{W}_{air\ turb} = \dot{m}_{air}(h_5 - h_6) \quad (39)$$

SI-ABC process was similar to ABC; the differences between the ABC gas turbine and SI-ABC were the HRSG and a mixer which provided steam for the bottoming cycle. The procedure is given in Flowchart 3 and 4 in the Appendix for ABC and SI-ABC.

2.6.1. Validation

To validate the model, the results of the model for ABC and SI-ABC were compared with those of the experiments performed by Ghazikhani et al. (Ghazikhani et al., 2011). Fig.17 displays variations of compression station overall efficiency with ABC or SI-ABC against TIT. SI-ABC system had more output power than ABC at the same bottoming cycle pressure ratio and TIT. This was due to more heat recovery in the regenerator in the SI-ABC cycles. It could produce exhaust with a lower temperature and more inlet mass to bottoming turbine. In addition, form Fig.17a good agreement between the model results and experimental data can be observed. The discrepancy between the two results was less than 4%.

2.6.2. Sensitivity Analysis

The effect of key parameters of process on its performance was evaluated by a sensitivity analysis. In Fig.18, the thermal efficiency of the ABCs and SI-ABCs varied against bottoming pressure ratio. The thermal efficiencies of steam injection system were higher than ABCs. Fig.19 shows, the efficiency reduces as the ambient temperature is increased. In addition, in the ABC, the reduction rate of efficiency with ambient temperature was steeper. In ABCs the effectiveness of the heat recovery in the bottom-cycle was also decreased by increasing ambient temperature due to a smaller difference between the two stream temperatures. Fig.19 also shows the superiority of the SI-ABC to have the highest efficiency in different ambient temperatures.

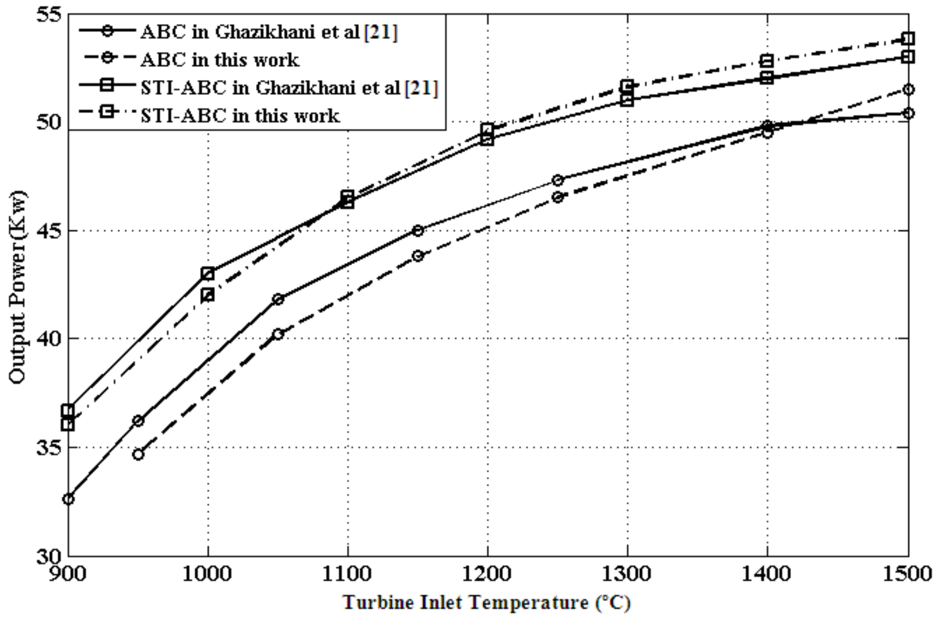

Figure 17. Comparison of Model Results with those of Ghazikhani et al. [17] for the ABC and SI-ABC

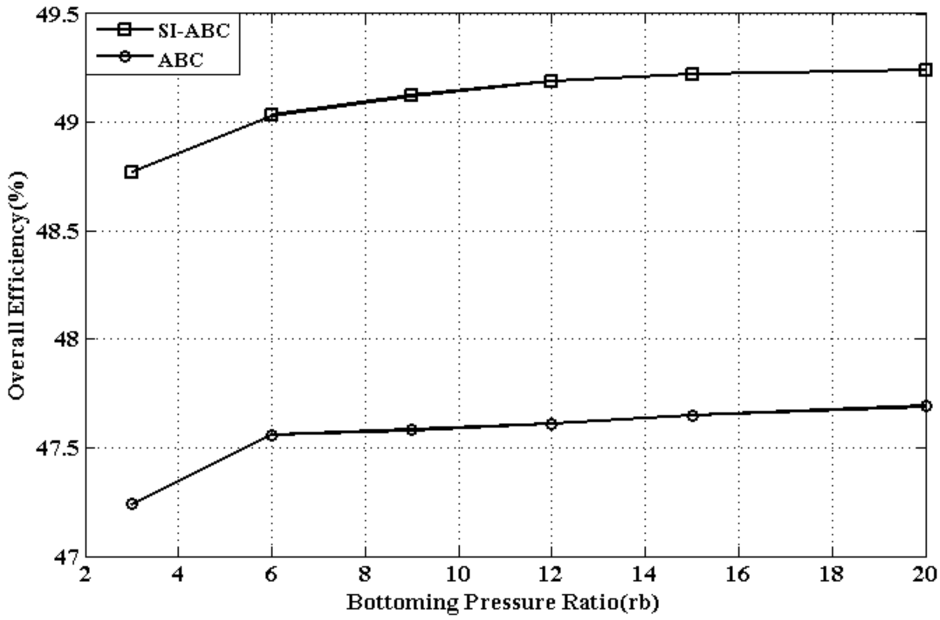

Figure 18. The Overall EfficiencyV against Pressure Ratio (TIT= 1400 °K, T0=25 °C)

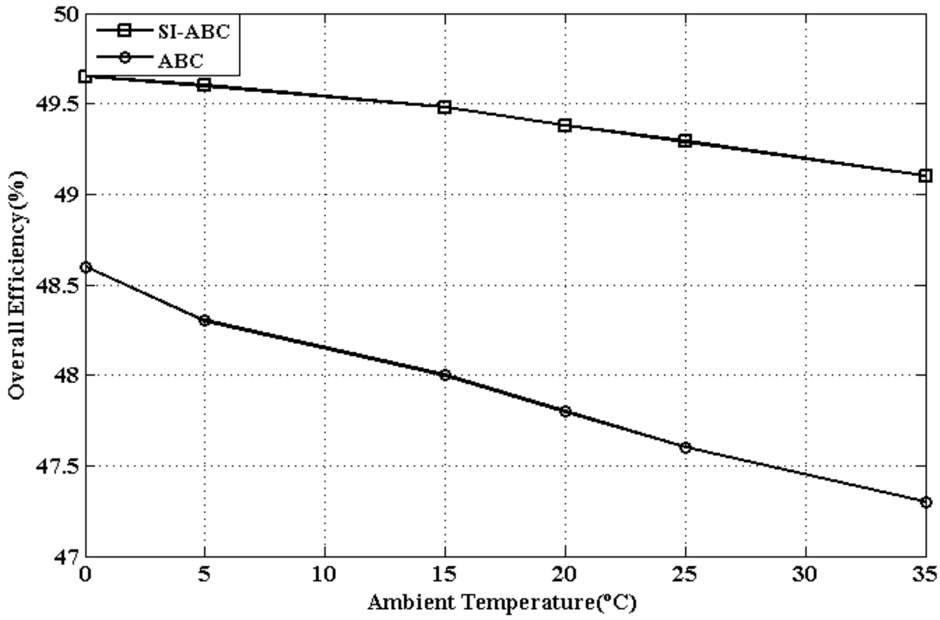

Figure 19. The Overall Efficiency Variation against Ambient Temperature (TIT= 1400 °K)

3. Results and Discussion

The proposed model was implemented for second Iranian gas pipeline network. Table 3 shows the properties of this network. In this network, the demand levels were different in different quarters of year. So it must be considered as an important variable which should be satisfied. In this regards, the model was evaluated for different demand levels. Optimization of the required power for the gas compressors in various demands was the first step in the minimizing of the total power consumption. Then the model used the energy recovery technologies within the pressure compression and reduction stations to estimate the improved overall efficiency and net output power. Table 4 displays the optimization results for simple network in the case study. The demand and the pressure ratio for all gas turbines was considered 50 MMSCMD and 14, respectively.

Having a clear comparison between the mentioned systems, the variation of gas transmission network overall efficiency against the demand, is shown in Fig.20. The comparison included six systems:

1. Simple pipeline
2. Simple pipeline with the turbo-expander in reduction stations
3. Simple pipeline with ABCs in compression stations and turbo-expander in reduction stations
4. Simple pipeline with SI-ABCs in compression stations and turbo-expander in reduction stations
5. Simple pipeline with ORC-butane in compression stations and turbo-expander in reduction stations
6. Simple pipeline with ORC-pentane in compression stations and turbo-expander in reduction stations

Fig.20 shows that the overall efficiency of the equipped transmission network by ORC-pentane and turbo-expander was higher than other systems at the same flow rate. These technologies increase the network overall efficiency 13-28 % in span of 50- 90 MMSCMD. As seen in the Fig.20, the overall efficiency of SI-ABCs was higher than ORC-butane at lower 65 MMSCMD. Although the effect of turbo expander on the overall efficiency was low at low flow rates, it had great impact on the efficiency at cold season when the demand level is high.

Fig.21 displays the increase of the overall efficiency with bottoming pressure ratio (rb) in the range of 5-15 for all systems. The flow rate was considered 70 MMSCMD. As seen in Fig.21, the overall efficiency of the ORC-pentane was more sensitive to bottoming pressure ratio than the other systems.

Table 3. The Characteristics of Iran Second Gas Transmission Network

Diameter (inch)	Designed maximum pressure (Kpa)	Designed minimum pressure (Kpa)	Number of compression stations	Number of reduction stations
56	8000	4000	7	9

Table 4. The Optimization Results for Compression Stations on Simple Pipeline

	Compression Station 1	Station 2	Station 3	Station 4	Station 5	Station 6	Station 7
P_{in} (Kpa)	4780	4343	4146	4147	4261	4160	4613
P_{out} (Kpa)	5258	4995	4768	4562	4687	4576	5074
Compressor power (Kw)	7931	9559	8530	5973	5476	4897	4172

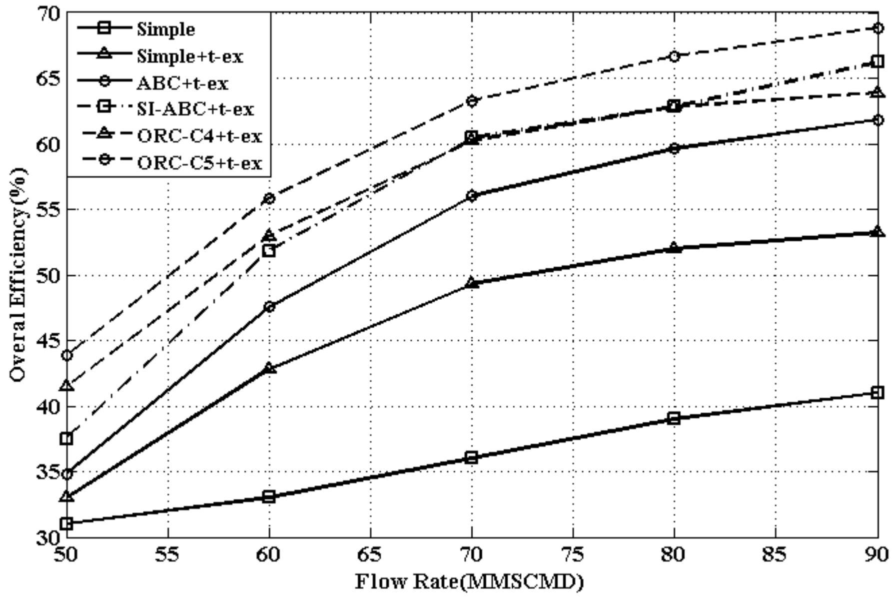

Figure 20. The Variation of Overall Efficiency of Iran`s Second Gas Pipeline against the Flow Rate

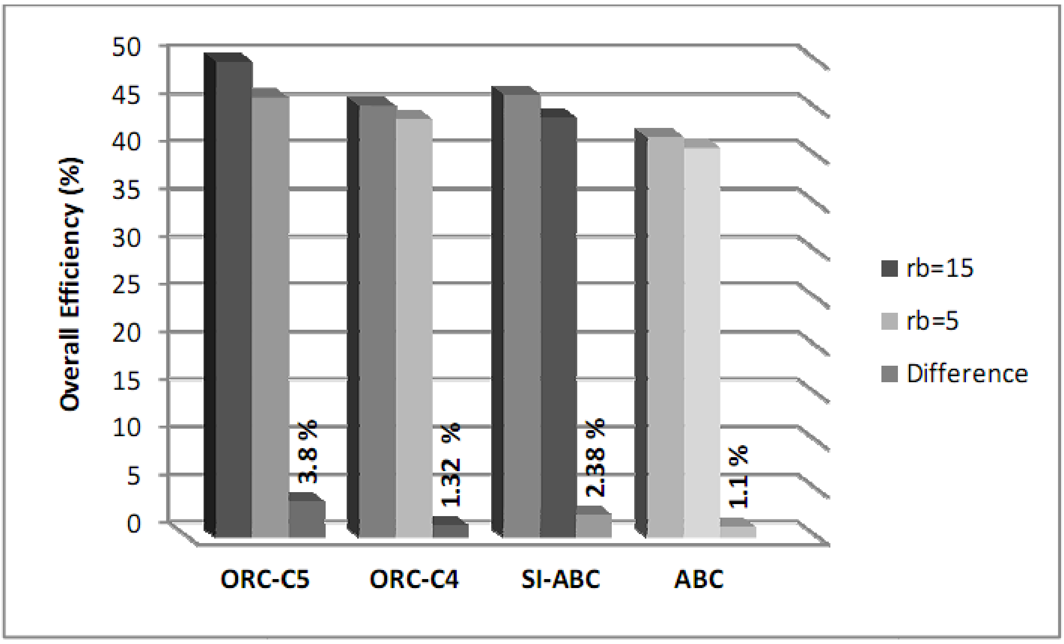

Figure 21. The Variation of Overall Efficiency of Gas Pipeline against the Bottoming Pressure Ratio in a Range of 5-15 (TIT= 1400 °K, T0=25 °C).

4. Conclusions

In this study, the effect of three technologies on the overall efficiency of gas transmission network was investigated. Based on an energy analysis a computer program was developed to survey improving the performance of gas transmission system. The examined technologies were organic rankine cycle, air bottoming cycle, and steam injection air bottoming cycle which were used in the pressure compression station and turbo-expander which was utilized within the pressure reduction stations.

The main conclusions were:

1) The turbo-expander outlet powers and required heat had a direct relationship with expander inlet pressure, temperature and flow-rate. In addition, when the inlet pressure ranged from 450 to 750 pisa and gas flow was maximum i.e. 866 MSCMH, the efficiency of the expander system was82-44%, respectively.

2) The SI-ABC was found to have maximum output power at the same bottoming cycle pressure ratio and turbine inlet temperature (TIT) in comparison with ABS. This was due to more heat recovery in the regenerator in the SI-ABC cycle that resulted a lower exhaust temperature; and more inlet mass to bottoming turbine causes a higher output work. Moreover, the results displayed that the overall efficiency was decreased as the ambient temperature had been increased for ABC and SI-ABC.

3) In this study, an organic rankine cycle using working fluid such as ammonia, butane, and water was analyzed and the results were compared together. When turbine inlet temperature varied from 90 to 135 (°C) the efficiency of ORCs with butane as working fluid decreased by 7.9 % averagely, although it increased by 7.2 % and 2.1 % for ammonia and water, respectively.

4) The ORC-pentane was more sensitive to variation of bottoming pressure ratio.

The model was tested for Iran second gas transmission network. The results showed that the highest efficiency is obtained from implementation of ORC with n-pentane as working fluid and turbo-expander in pressure compression and reduction stations, respectively. The demand or gas flow rate through pipeline was the most effective parameter that needed to satisfy. So, variation of the transmission system overall efficiency was investigated based on the flow rate.

When the study network was equipped by ORC-pentane and turbo-expander, the overall efficiency grew by 22 % averagely, in the span of 50 to 90 MMSCMD.

Appendices

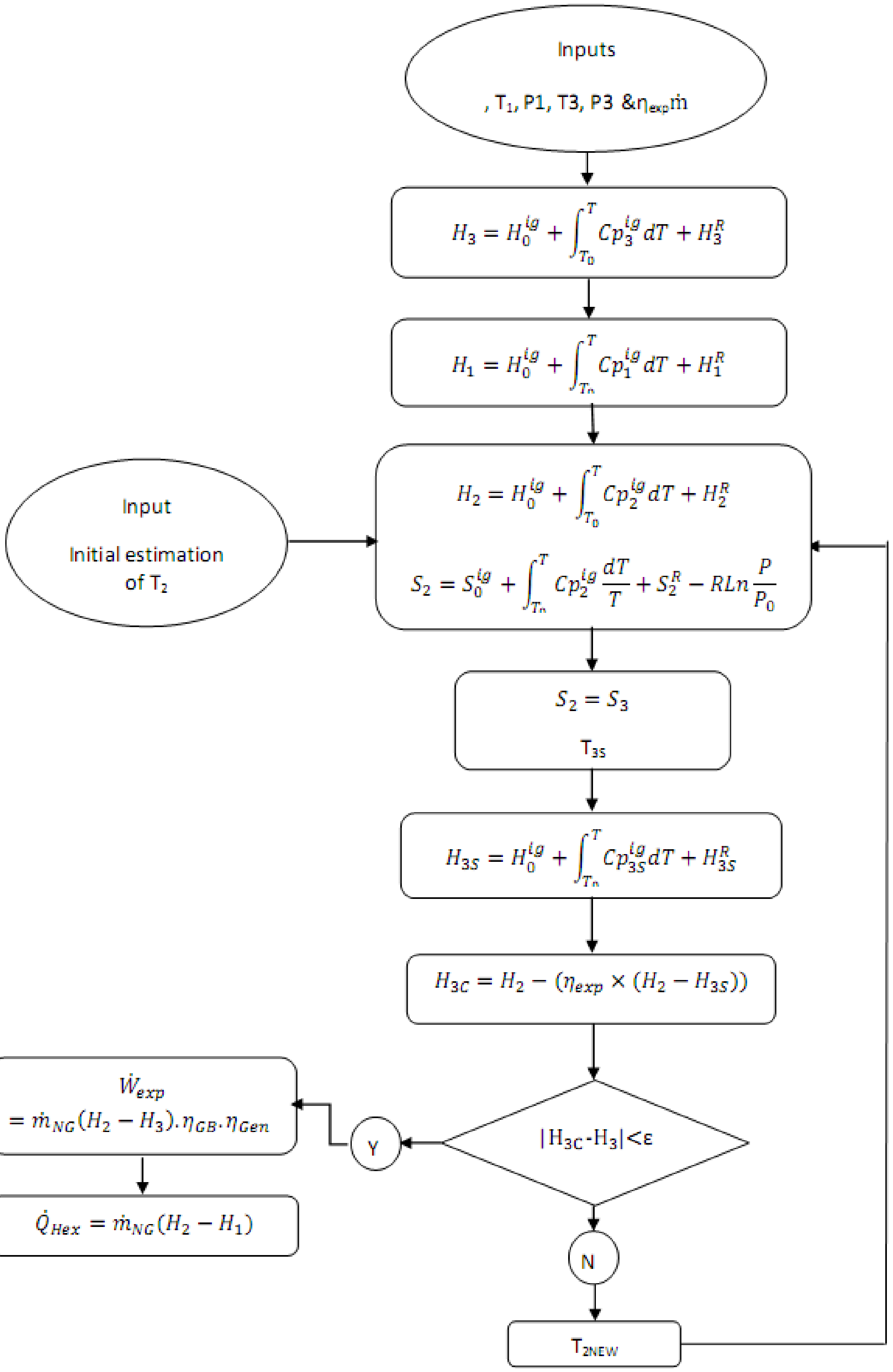

Flowchart 1. Turbo-Expander Calculation

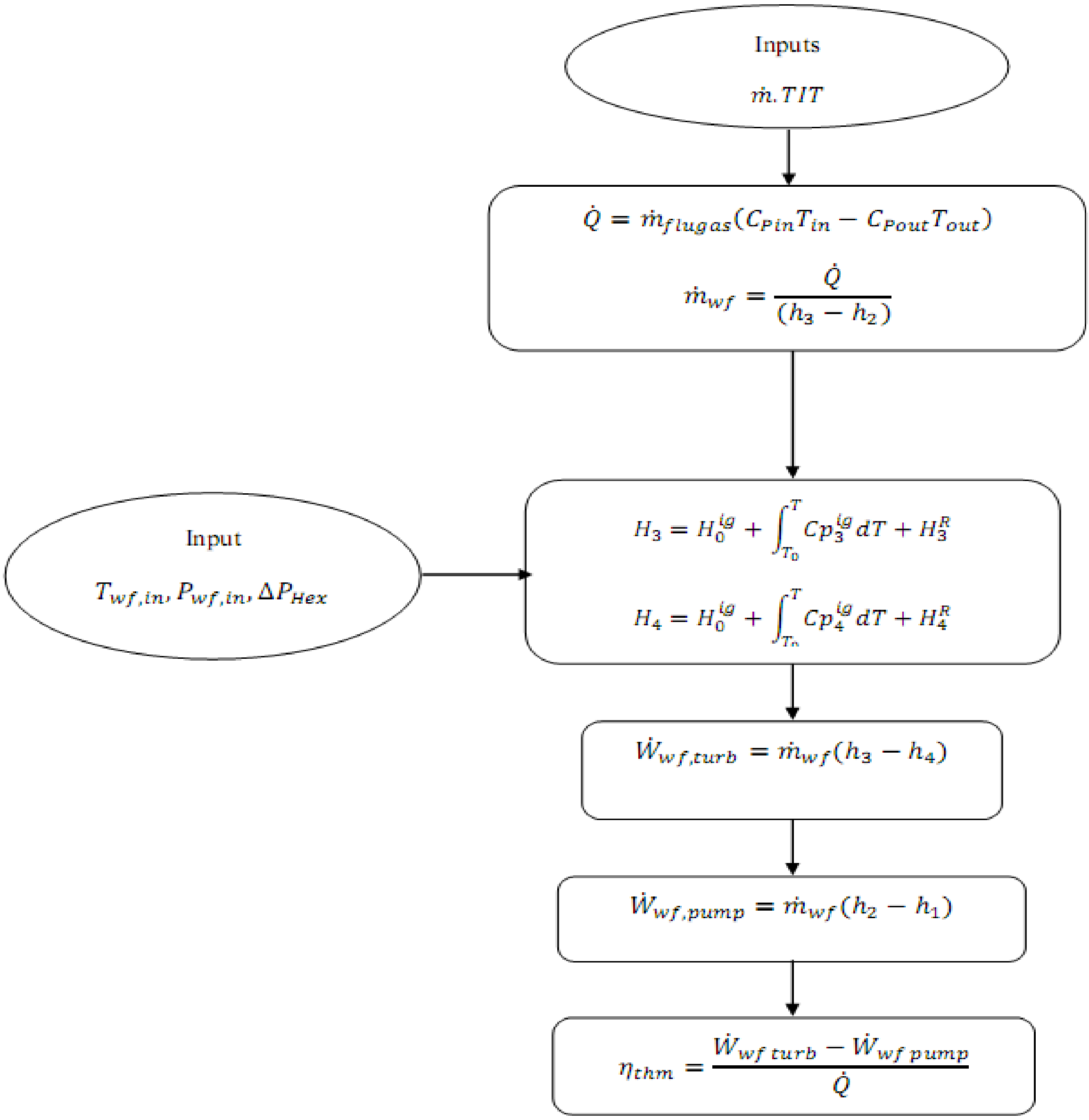

Flowchart 2. ORCs Calculation

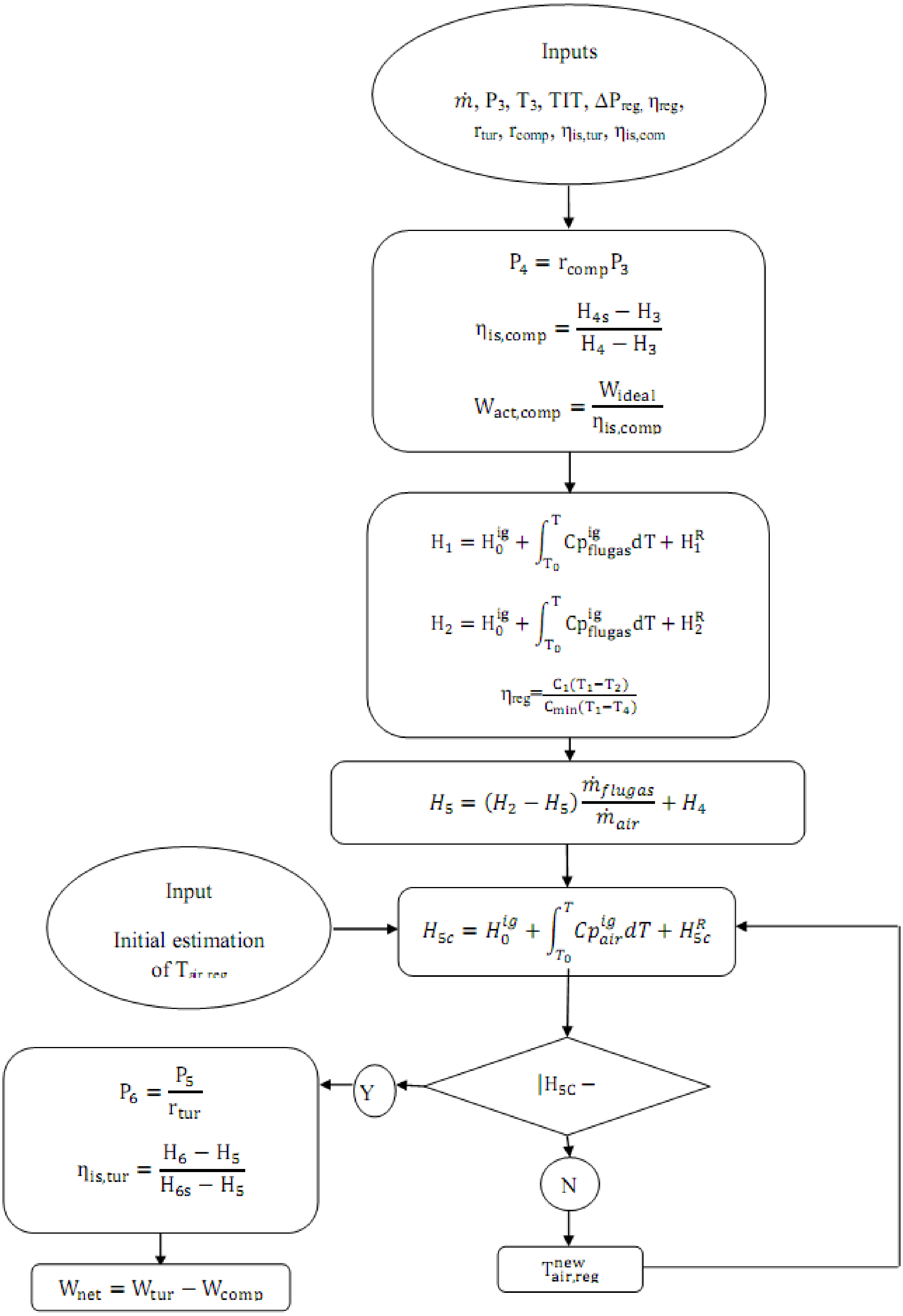

Flowchart 3. ABCs Calculation

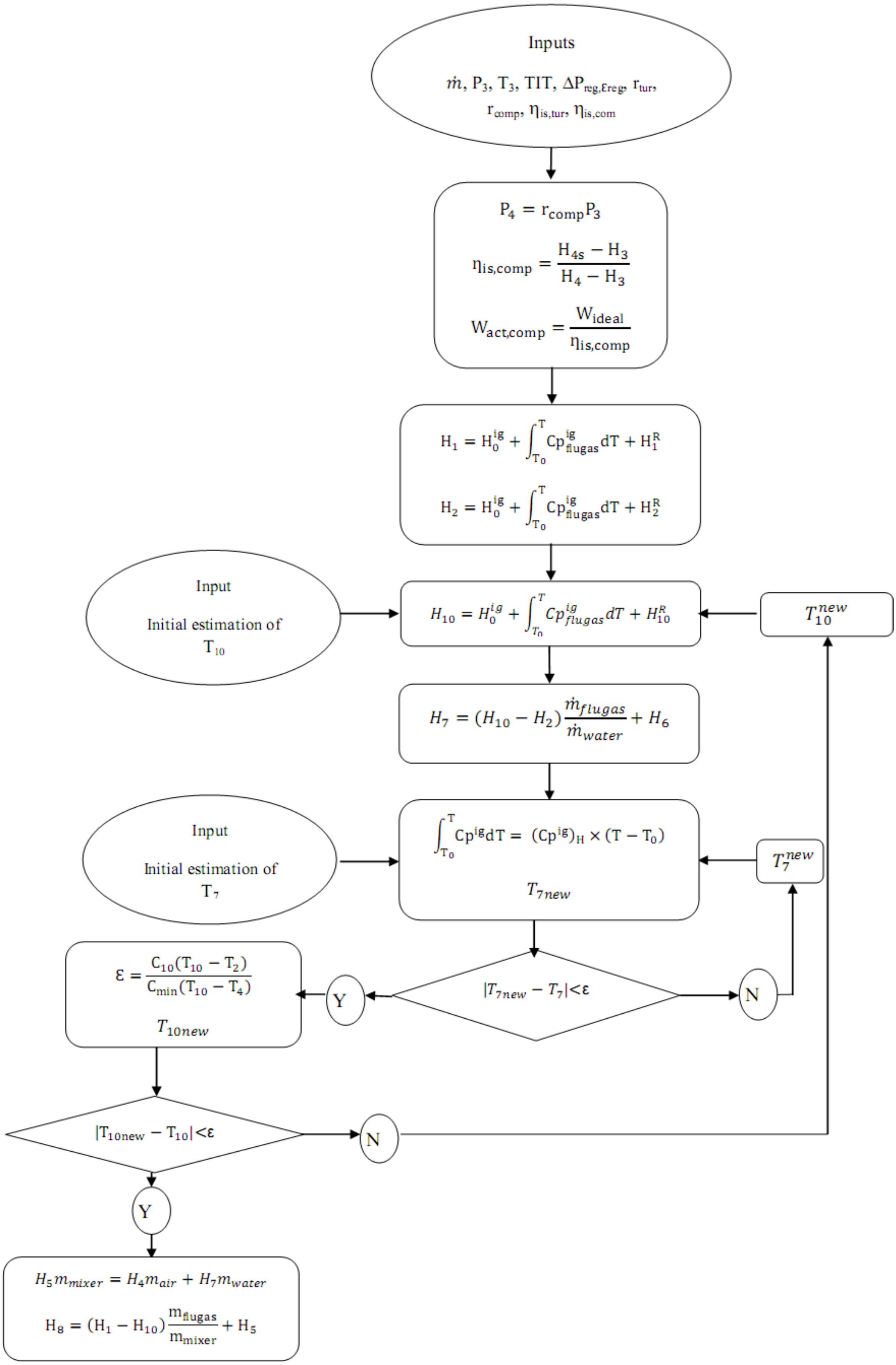
Inputs
$\dot{m}$, P_3, T_3, TIT, $\Delta P_{reg,\varepsilon reg}$, r_{tur}, r_{comp}, $\eta_{is,tur}$, $\eta_{is,com}$
$P_4 = r_{comp} P_3$
$\eta_{is,comp} = \frac{H_{4s} - H_3}{H_4 - H_3}$
$W_{act,comp} = \frac{W_{ideal}}{\eta_{is,comp}}$
$H_1 = H_0^{ig} + \int_{T_0}^{T} Cp_{flugas}^{ig} dT + H_1^R$
$H_2 = H_0^{ig} + \int_{T_0}^{T} Cp_{flugas}^{ig} dT + H_2^R$
Input
Initial estimation of T_{10}
$H_{10} = H_0^{ig} + \int_{T_0}^{T} Cp_{flugas}^{ig} dT + H_{10}^R$
T_{10}^{new}
$H_7 = (H_{10} - H_2)\frac{\dot{m}_{flugas}}{\dot{m}_{water}} + H_6$
Input
Initial estimation of T_7
$\int_{T_0}^{T} Cp^{ig} dT = (Cp^{ig})_H \times (T - T_0)$
T_{7new}
T_7^{new}
$|T_{7new} - T_7| < \varepsilon$
Y
N
$\varepsilon = \frac{C_{10}(T_{10} - T_2)}{C_{min}(T_{10} - T_4)}$
T_{10new}
$|T_{10new} - T_{10}| < \varepsilon$
N
Y
$H_5 m_{mixer} = H_4 m_{air} + H_7 m_{water}$
$H_8 = (H_1 - H_{10})\frac{m_{flugas}}{m_{mixer}} + H_5$

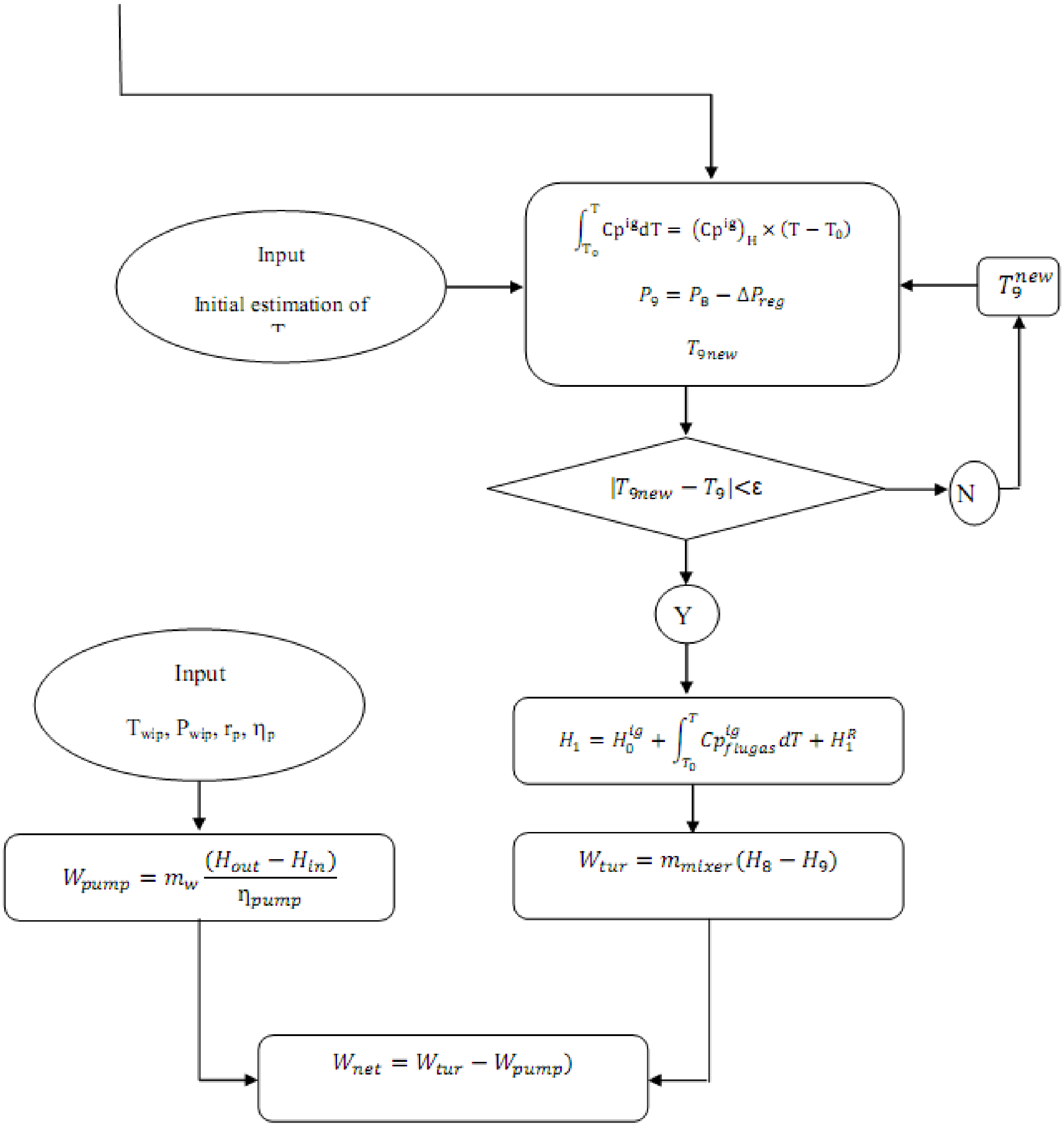

Flowchart 4. SI- ABCs Calculation

Nomenclature

ABC	air bottoming cycle
AC	air compressor
CC	combustion chamber
Cp^{ig}	ideal gas specific heat (kJ/kgmol.K)
C4	Butane
C5	Pentane
GC	gas compressor
GT	gas turbine
h	specific enthalpy (kJ/ kgmol)
H	enthalpy (kJ)
HRSG	heat recovery steam system
M	mass flow rate (kg/s)
MSCMD	Million standard cubic meter per day
MSCMH	Million standard cubic meter per hour
ORC	organic rankine cycle
P	Pressure (kPa)
Q	volume flow of natural gas (MSCMH)
Q_{Hex}	heat duty (kW)
Rb	bottoming pressure ratio
R	specific-gas constant (kJ /kg.K)
S	specific entropy (kJ /kg.K)
S	entropy(kJ/K)
SI-ABC	steam injection ABC
T0	ambient temperature (K)
TIT	turbine inlet temperature (˚C)
W	acentric factor
W	work (kW)
Z	compressibility factor
E	heater effectiveness factor
H	Efficiency

References

Abbott, M. M., Smith, J. M., & Van Ness, H. C. (2001). Introduction to chemical engineering thermodynamics. *McGraw-Hill.*

Bolland, O., Forde, M., & Hande, B. (1996). Air bottoming cycle: use of gas turbine waste heat for power generation. *Journal of engineering for gas turbines and power, 118*(2), 359-368.

Borraz-Sánchez, C., & Ríos-Mercado, R. Z. (2005). A hybrid meta-heuristic approach for natural gas pipeline network optimization *Hybrid Metaheuristics* (pp. 54-65): Springer.

Cho, S.-Y., Cho, C.-H., & Kim, C. (2008). Performance characteristics of a turbo expander substituted for expansion valve on air-conditioner. *Experimental Thermal and Fluid Science, 32*(8), 1655-1665.

Dai, Y., Wang, J., & Gao, L. (2009). Parametric optimization and comparative study of organic Rankine cycle (ORC) for low grade waste heat recovery. *Energy Conversion and Management, 50*(3), 576-582.

Desai, N. B., & Bandyopadhyay, S. (2009). Process integration of organic Rankine cycle. *Energy, 34*(10), 1674-1686.

Drescher, U., & Brüggemann, D. (2007). Fluid selection for the Organic Rankine Cycle (ORC) in biomass power and heat plants. *Applied Thermal Engineering, 27*(1), 223-228.

Edgar, T., Himmelblau, D., & Bickel, T. (1978). Optimal design of gas transmission networks. *Society of Petroleum Engineers Journal, 18*(02), 96-104.

Ghazikhani, M., Passandideh-Fard, M., & Mousavi, M. (2011). Two new high-performance cycles for gas turbine with air bottoming. *Energy, 36*(1), 294-304.

Guo, B., & Ghalambor, A. (2014). *Natural gas engineering handbook*: Elsevier.

Kabirian, A., & Hemmati, M. R. (2007). A strategic planning model for natural gas transmission networks. *Energy policy, 35*(11), 5656-5670.

Kambanis, L. M. T. (1995). *Analysis and modeling of power transmitting systems for advanced marine vehicles.* Massachusetts Institute of Technology.

Korobitsyn, M. A. (1998). *New and Advanced Conversion Technologies: Analysis of Cogeneration, Combined and*

Integrated Cycles: University of Twente.

Larjola, J. (1995). Electricity from industrial waste heat using high-speed organic Rankine cycle (ORC). *International journal of production economics, 41*(1), 227-235.

Maddaloni, J. D., & Rowe, A. M. (2007). Natural gas exergy recovery powering distributed hydrogen production. *International journal of hydrogen energy, 32*(5), 557-566.

Menon, E. S. (2005). *Gas pipeline hydraulics*: CRC Press.

Najibi, H., & Taghavi, N. (2011). Effect of different parameters on optimum design for high pressure natural gas trunk-lines. *Journal of Natural Gas Science and Engineering, 3*(4), 547-554.

Nishada, K., Takagi, T., & Kinoshita, S. (2005). Regenerative steam injection gas turbine system. *Applied Energy, 81*, 231-246.

O'Neill, R. P., Williard, M., Wilkins, B., & Pike, R. (1979). A mathematical programming model for allocation of natural gas. *Operations Research, 27*(5), 857-873.

Poživil, J. (2004). Use of expansion turbines in natural gas pressure reduction stations. *Acta Montanistica Slovaca, 3*(9), 258-260.

Ríos-Mercado, R. Z., Kim, S., & Boyd, E. A. (2006). Efficient operation of natural gas transmission systems: A network-based heuristic for cyclic structures. *Computers & Operations Research, 33*(8), 2323-2351.

Roy, J., Mishra, M., & Misra, A. (2010). Parametric optimization and performance analysis of a waste heat recovery system using Organic Rankine Cycle. *Energy, 35*(12), 5049-5062.

Safarian, S., & Aramoun, F. (2015). Energy and exergy assessments of modified Organic Rankine Cycles (ORCs). *Energy Reports, 1*, 1-7.

Safarian, S., & Bararzadeh, M. (2012). Exergy analysis of high-performance cycles for gas turbine with air-bottoming. *Journal of Mechanical Engineering Research, 5*(2), 38-49.

Safarian, S., Saboohi, Y., & Kateb, M. (2013). Evaluation of energy recovery and potential of hydrogen production in Iranian natural gas transmission network. *Energy policy, 61*, 65-77.

Vaja, I., & Gambarotta, A. (2010). Internal combustion engine (ICE) bottoming with organic Rankine cycles (ORCs). *Energy, 35*(2), 1084-1093.

Wei, D., Lu, X., Lu, Z., & Gu, J. (2007). Performance analysis and optimization of organic Rankine cycle (ORC) for waste heat recovery. *Energy Conversion and Management, 48*(4), 1113-1119.

Wu, S., Rios-Mercado, R. Z., Boyd, E. A., & Scott, L. R. (2000). Model relaxations for the fuel cost minimization of steady-state gas pipeline networks. *Mathematical and Computer Modelling, 31*(2), 197-220.

Zaleta, D., & Ríos-Mercado, R. (2002). A MINLP Model for a Minimizing Fuel Consumption on Natural Gas Pipeline Networks: October.